Spin Squeezing by Rydberg Dressing in an Array of Atomic Ensembles

Jacob A. Hines, Shankari V. Rajagopal, Gabriel L. Moreau, Michael D. Wahrman, Neomi A. Lewis, Ognjen Marković, and Monika Schleier-Smith

Phys. Rev. Lett. **131**, 063401 — Published 10 August 2023

DOI: 10.1103/PhysRevLett.131.063401

Spin Squeezing by Rydberg Dressing in an Array of Atomic Ensembles

Jacob A. Hines,[1] Shankari V. Rajagopal,[1] Gabriel L. Moreau,[1] Michael D. Wahrman,[2]
Neomi A. Lewis,[2] Ognjen Marković,[1,3] and Monika Schleier-Smith[1]

[1] *Department of Physics, Stanford University, Stanford, California 94305, USA*
[2] *Department of Applied Physics, Stanford University, Stanford, California 94305, USA*
[3] *Department of Physics, Harvard University, Cambridge, MA 02138, USA*

(Dated: June 9, 2023)

We report on the creation of an array of spin-squeezed ensembles of cesium atoms via Rydberg dressing, a technique that offers optical control over local interactions between neutral atoms. We optimize the coherence of the interactions by a stroboscopic dressing sequence that suppresses super-Poissonian loss. We thereby prepare squeezed states of $N = 200$ atoms with a metrological squeezing parameter $\xi^2 = 0.77(9)$ quantifying the reduction in phase variance below the standard quantum limit. We realize metrological gain across three spatially separated ensembles in parallel, with the strength of squeezing controlled by the local intensity of the dressing light. Our method can be applied to enhance the precision of tests of fundamental physics based on arrays of atomic clocks and to enable quantum-enhanced imaging of electromagnetic fields.

Quantum projection noise limits the precision of state-of-the-art measurements of time, acceleration, and electromagnetic fields based on spectroscopy of ensembles of atoms. Entanglement among the constituent two-state atoms, or equivalently spins, can enable enhanced precision by squeezing the quantum noise [1–3]. Spin squeezing has been demonstrated in several experimental platforms featuring all-to-all interactions, including atoms in optical cavities [4–7], Bose-Einstein condensates [8–15], and ions coupled by collective motion [16, 17]. However, a wide range of metrological tasks stand to benefit from instead generating spin squeezing with local interactions. Notably, entangling Rydberg atoms [18–29], molecules [30], or solid-state spins [31, 32] via their native interactions offers prospects for applying squeezing in optical tweezer clocks [33, 34], electrometers [35], molecular spectroscopy [30], and compact magnetometers [36].

For local control of spin squeezing in systems of neutral atoms, several proposals have envisioned applying the method of Rydberg dressing [24, 27–29, 37]. Here, an off-resonant laser field hybridizes one of two ground spin states with a Rydberg state to induce interactions with a characteristic range on the few-micron scale [38–40]. Such short-range interactions are ideally suited to generating arrays of independent squeezed states for spatially resolved sensing [15]. By offering local and dynamical optical control [41, 42], Rydberg dressing further promises to enable metrological protocols employing multiple internally entangled ensembles to maximize the dynamic range of a sensor or the stability of a clock [43–45].

Several experiments have demonstrated coherent Rydberg-dressed interactions in small systems [19, 20, 46, 47]. However, maintaining sufficient coherence to scalably engineer many-body entanglement has so far proven challenging [42, 48–50]. Decoherence is dominated by facilitated excitation, wherein a single atom that decays into a Rydberg state shifts the atomic transition for surrounding atoms into resonance with the dressing light, triggering an avalanche of subsequent excitations [48, 49, 51–53]. This effect is of greatest issue in systems with high dimensionality, such as 3D optical lattices [48, 50] and bulk gases [49]. These systems are particularly relevant in metrological applications, where increased particle number enables increased measurement precision.

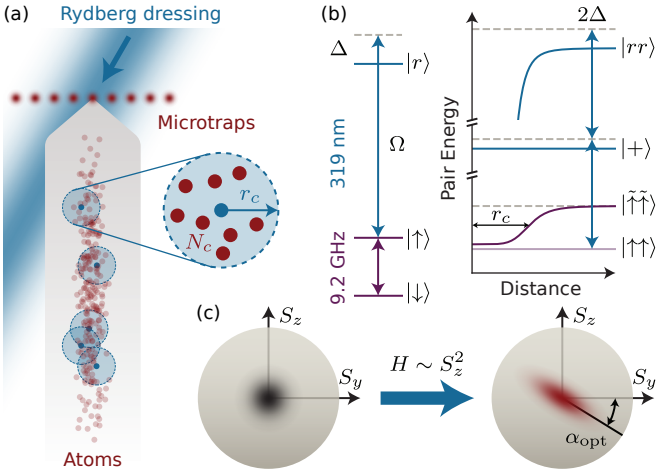

FIG. 1. **Experimental setup**. (a) An array of atomic ensembles is locally illuminated with 319 nm Rydberg dressing light, inducing interactions of characteristic range r_c. (b) Level diagrams for one atom (left) and a pair of atoms (right), where $|+\rangle = (|r\uparrow\rangle + |\uparrow r\rangle)/\sqrt{2}$ and $|\tilde{\uparrow}\rangle$ denotes the Rydberg-dressed state. (c) Interactions generate an S_z-dependent precession (twisting) of the collective spin S that shears a coherent state (left) into a squeezed spin state (right).

In this Letter, we report on the generation of an array of spin-squeezed atomic ensembles by Rydberg dressing. For pseudospins encoded in the hyperfine clock states of cesium, we generate Ising interactions by off-resonantly coupling one clock state to a Rydberg state. Whereas applying the dressing light continuously induces super-

Poissonian loss attributable to avalanche effects, a stroboscopic pulse sequence suppresses this loss to enable coherent interactions. We observe the dependence of the resulting squeezing on the local intensity of the dressing light and detect squeezing in three adjacent ensembles, with a minimum metrological squeezing parameter $\xi^2 = 0.77(9)$.

Our experiments are conducted in a one-dimensional array of optical microtraps [Fig. 1(a)], consisting of nine sites with 25 μm spacing. Each array site contains a cloud of typically $N = 200$ cesium atoms with rms dimensions [1.7(2), 1.7(2), 19(2)] μm, corresponding to a peak density $\rho_0 = 2.3(3) \times 10^{11}$ cm^{-3}. We prepare the atoms in a superposition of the hyperfine clock states $|\downarrow\rangle = \left|6S_{1/2}, F = 3, m_F = 0\right\rangle$ and $|\uparrow\rangle = \left|6S_{1/2}, F = 4, m_F = 0\right\rangle$. To introduce Ising interactions within each array site, we dress the state $|\uparrow\rangle$ using 319 nm light detuned by an amount Δ from the $60P_{3/2}$ Rydberg state $|r\rangle$ [Fig. 1(b)]. A nonuniform intensity of the dressing light across the array allows us to perform experiments at multiple Rabi frequencies Ω in parallel.

The interactions induced by Rydberg dressing can be understood as a suppression of the ac Stark shift that the dressing light imparts to each atom due to the influence of nearby atoms [Fig. 1(b)]. This effect is most pronounced for an ensemble of N atoms localized within a critical length scale $r_c \approx |C_6/2\Delta|^{1/6}$, below which the van der Waals interaction $V_{\mathrm{R}} = C_6/r^6$ between two Rydberg atoms exceeds the pair-state detuning 2Δ. In this idealized limit, the Hamiltonian takes the form

$$H \approx U_0 S_z - \frac{\chi}{N} S_z^2, \tag{1}$$

where $S_z = (N_\uparrow - N_\downarrow)/2$ denotes the population difference between the clock states [24]. Here, $U_0 \approx \Omega^2/(4\Delta)$ denotes an overall ac Stark shift that can readily be removed by spin echo, while $\chi \approx N\Omega^4/(16\Delta^3)$ parameterizes the mean-field interaction, which manifests in an S_z-dependence of the ac Stark shift. The resulting S_z-dependent spin precession, termed one-axis twisting [1], provides a means of squeezing quantum fluctuations [Fig. 1(c)].

Our experiment is guided by this idealized model of spin squeezing by one-axis twisting but must contend with two key factors beyond it. Firstly, we operate with atomic clouds larger than the interaction ellipsoid with radii $r_c^{x,y,z} \approx (3, 5, 5)$ μm, so the collective spin model in Eq. 1 only approximately describes the dynamics [54]. Secondly, the squeezing must compete with decay of the Rydberg-dressed state, which in practice is often exacerbated by multi-body loss processes that induce super-Poissonian noise [48–50]. We focus first on minimizing such loss to optimize the coherence of the dressing, before examining the role of the finite interaction range and observing the resulting squeezing.

We maximize coherence in our system by implementing a stroboscopic dressing sequence designed to suppress facilitated excitation to the Rydberg state [Fig. 2(a-b)]. We apply the dressing light in a sequence of pulses, each smoothly shaped to ensure that the dressing is adiabatic and ideally leaves all atoms in the ground state $|\uparrow\rangle$ at the end of the pulse. Non-idealities, including incoherent excitation due to laser phase noise and blackbody decay to nearby Rydberg S and D states that are dipole-coupled to the dressing state $|r\rangle$, can nevertheless lead to atoms populating the Rydberg manifold. A separation τ_d between the pulses provides time for any contaminant atoms to decay or be expelled by antitrapping, thereby averting avalanche effects. Such stroboscopic dressing was proposed in Refs. [20, 50] and implemented in Ref. [41] for measurements of mean-field dynamics.

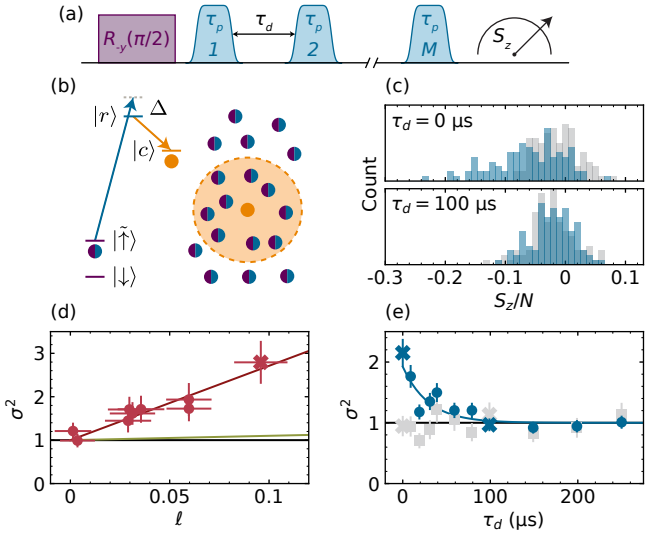

FIG. 2. **Stroboscopic Rydberg dressing**. (a) An equal superposition of states $|\uparrow\rangle$ and $|\downarrow\rangle$ is prepared by a $\pi/2$ microwave rotation (purple) and subjected to dressing pulses of length τ_p (blue) at intervals τ_d. (b) Atoms in contaminant states $|c\rangle$ (orange) influence dressed atoms $|\tilde{\uparrow}\rangle$ (purple-blue). (c) Histograms of S_z for one microtrap with (blue) or without (gray) dressing light. Broadening observed for continuous dressing (top, $\tau_d = 0$) is suppressed by pulse delay $\tau_d = 100$ μs (bottom). (d) Normalized variance vs loss, plotted across microtraps for $\tau_d = 0$ μs. Linear fit (red) reports atoms being lost in groups of size $g = 17(1)$. Green shows Poissonian loss ($g = 1$). (e) Normalized variance, averaged across three central microtraps, vs pulse delay for $\tau_p = 628$ ns, $M = 48$. Fitting to $\sigma^2 = A\exp(-\gamma\tau_d) + 1$ yields $\gamma^{-1} = 29(9)$ μs. "×" markers in (d-e) denote data shown in (c).

For spin squeezing, optimization of the dressing pulse sequence is essential to avoiding even subtle loss processes that add percent-level noise to the quantum state. To probe such loss, we first prepare each atom in an equal superposition state $|\pi/2\rangle = (|\uparrow\rangle + |\downarrow\rangle)/\sqrt{2}$, obtained by a $\pi/2$ microwave rotation of the initial state $|\downarrow\rangle$ [Fig. 2(a)]. We then apply a sequence of dressing pulses separated by a variable time τ_d. Since the dressing light affects only

state $|\uparrow\rangle$, any light-induced loss manifests in a population difference between the two spin states, which we read out by state-sensitive fluorescence imaging.

Figure 2(c) shows representative histograms of the population imbalance S_z/N between the clock states in a single microtrap after a total dressing time $\tau_{\rm int} = 30$ μs. For light applied in a single long pulse ($\tau_d = 0$), we observe loss from state $|\uparrow\rangle$ and accompanying noise in the atomic state populations. Performing the same analysis for all microtraps, which experience different levels of loss due to the spatially varying light intensity, we plot the spin noise versus loss in Fig. 2(d). Specifically, we define $\sigma^2 = 4(\Delta S_z)^2/N$ as the variance normalized to that of a coherent spin state and plot σ^2 as a function of the fractional loss $\ell = (\langle S_z\rangle_0 - \langle S_z\rangle)/N$, where $\langle S_z\rangle_0 \approx 0$ is the population imbalance in the absence of dressing light. For small loss ℓ, we observe a growth $\sigma^2 \approx 1 + g\ell$, where the slope $g = 17(1)$ exceeding unity evidences super-Poissonian statistics.

The loss is suppressed by introducing a delay between the dressing pulses. In particular, we divide the total dressing time $\tau_{\rm int}$ into $M = 48$ pulses spaced by a variable delay. The histogram of the state populations after dressing with delay $\tau_d = 100$ μs [Fig. 2(c)] exhibits substantially reduced loss and negligible broadening. Plotting the dependence of the spin noise σ^2 on the delay τ_d [Fig. 2(e)] reveals that the noise decays to the quantum projection noise level $\sigma^2 = 1$ on a characteristic timescale $\gamma^{-1} = 29(9)$ μs. We attribute this timescale to a combination of the Rydberg atoms' radiative decay and ejection out of the microtraps via the repulsive ponderomotive force, both of which occur on times of order 100 μs [54, 55]. We henceforth set $\tau_d = 100$ μs to ensure negligible broadening of the S_z distribution.

Observing the interactions induced by Rydberg dressing requires measuring the S_z-dependent phase accrual due to the dressing light. Specifically, the dressing light shifts the clock transition of each atom by an amount

$$U = \frac{\Omega^2}{4\Delta}\cdot\frac{1}{\sqrt{1+N_c^{\uparrow}\,(\Omega/\Delta)^2}}, \tag{2}$$

in units where $\hbar = 1$. Here $N_c^{(\uparrow)}$ denotes the number of surrounding atoms (in state $|\uparrow\rangle$) within the interaction ellipsoid of radii $r_c(\Delta)$. In the ideal case where all atoms are confined within the interaction range ($N_c = N$), expanding Eq. 2 in powers of $S_z = N_c^{\uparrow} - N_c/2$ yields the one-axis twisting Hamiltonian (Eq. 1). More generally, we expect similar twisting dynamics [24, 41, 54] with a collective interaction strength χ set by the number of neighbors N_c as

$$\chi = -\left(\frac{N}{2}\frac{dU}{dS_z}\right)_{S_z=0} = \frac{N_c}{16}\frac{\Omega^4}{\tilde{\Delta}^3}, \tag{3}$$

where $\tilde{\Delta} = \sqrt{\Delta^2 + N_c\Omega^2/2}$.

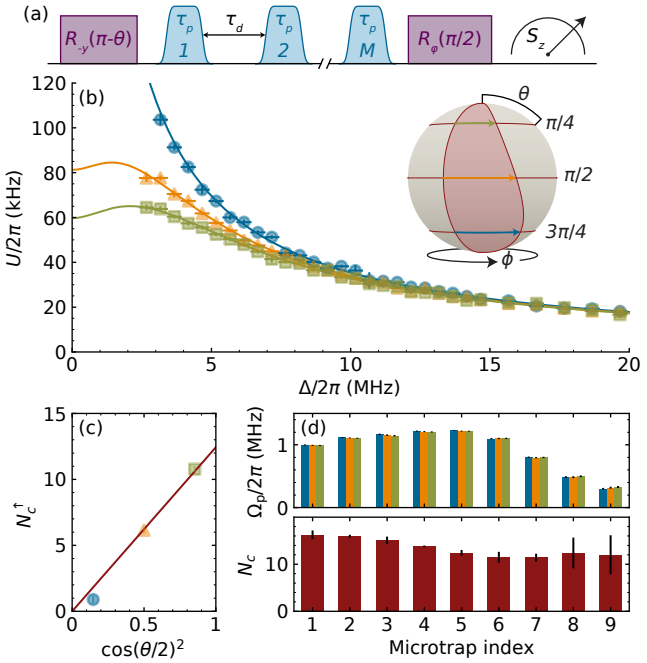

FIG. 3. **Quantifying interactions**. (a) Microwave (purple) and dressing (blue) pulse sequence for measuring the ac Stark shift U by Ramsey spectroscopy. (b) $U(\Delta)$ measured at $\theta = (\pi/4, \pi/2, 3\pi/4)$ (green squares, orange triangles, blue circles). Solid lines show fits that determine $\Omega_{\rm p}$ and $N_c^{\uparrow}$. Inset: visualization of accumulated phase ϕ. (c) $N_c^{\uparrow}(\Delta_*)$ vs $\cos^2(\theta/2)$, with linear fit (red line) of slope N_c. (d) Fitted number of neighbors (bottom) and Rabi frequency (top).

To experimentally determine the number of interacting neighbors and the collective interaction strength, we measure the ac Stark shift for atoms prepared in different initial states $|\theta\rangle = \cos(\theta/2)\,|\uparrow\rangle + \sin(\theta/2)\,|\downarrow\rangle$. We perform each measurement via the Ramsey sequence shown in Fig. 3(a), where stroboscopic dressing is followed by a $\pi/2$ microwave rotation that converts the acquired phase into a measurable population difference. Based on the total phase shift $\phi = \int U(t)\,dt$ measured in the Ramsey sequence and the known shape of the dressing pulse, we determine the ac Stark shift U [54]. The dependence of U on detuning Δ is shown in Fig. 3(b) for three different polar angles $\theta = (\pi/4, \pi/2, 3\pi/4)$ of the collective Bloch vector. The suppression of the ac Stark shift with decreasing polar angle evidences interactions among the Rydberg-dressed atoms in state $|\uparrow\rangle$.

We quantify the interactions by fitting the dependence of the ac Stark shift U on detuning. These fits reveal [54] both the peak Rabi frequency $\Omega_{\rm p}$ and the number of interacting neighbors $N_c^{\uparrow} \propto \rho\cos^2(\theta/2)\prod_\alpha r_c^\alpha(\Delta)$ for each microtrap. The data corroborate the expected dependence $N_c^{\uparrow} \propto \cos^2(\theta/2)$ of the number of interacting neighbors on the tilt of the Bloch vector, shown in Fig. 3(c) for a representative detuning $\Delta_* = 2\pi \times 8$ MHz. Linear fits of the form $N_c^{\uparrow} = N_c\cos^2(\theta/2)$ reveal the total number

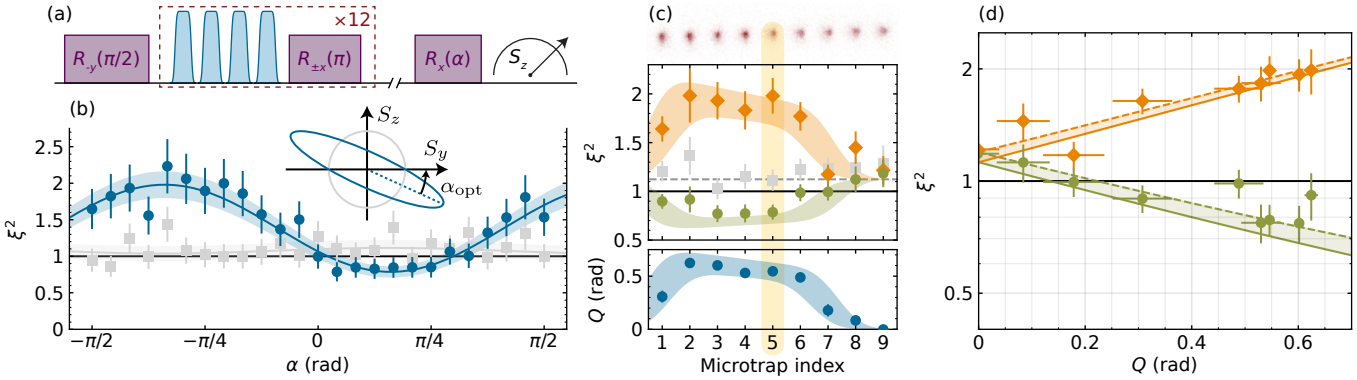

FIG. 4. **Spin squeezing**. (a) Sequence of microwave (purple) and dressing (blue) pulses for preparing the initial state $|\pi/2\rangle$, implementing one-axis twisting with spin echo, and measuring S_α. (b) Squeezing parameter ξ^2 vs α for one microtrap, measured with (blue circles) and without (gray squares) dressing. (c) Top: minimum ($\xi^2_{\rm min}$, green circles) and maximum ($\xi^2_{\rm max}$, orange diamonds) squeezing parameters after dressing. Bottom: twisting strength Q (blue circles). Gray squares represent $\xi^2(\alpha_{\rm opt})$ with no dressing light. Gray dotted line denotes $\mathcal{C}_0^{-2}$. Blue shaded region is a guide to the eye for the twisting strength used to predict squeezing (orange shaded) and antisqueezing (green shaded). Yellow shading indicates microtrap shown in (b). Top: fluorescence image of microtraps. (d) Squeezing (green circles) and antisqueezing (orange diamonds) vs Q. Solid lines denote parameter-free model of one-axis twisting for N_c atoms with initial contrast $\mathcal{C}_0$. Dotted lines add 7% technical noise, consistent with excess noise observed without dressing in (c).

of neighbors N_c within the interaction ellipsoid in each microtrap [Fig. 3(d)]. The result of $N_c \approx 13$ neighbors, approximately consistent with the atomic density and the calculated Rydberg-dressed potential [54], confirms that the total system size is $N/N_c \approx 15$ times larger than the interaction ellipsoid, as illustrated in Fig. 1(a).

To generate spin squeezing, we apply stroboscopic Rydberg dressing to an initial spin-polarized state $|\theta\rangle = |\pi/2\rangle$ along $\hat{\mathbf{x}}$. We isolate the twisting effect of the Ising term in Eq. 1 by a spin echo sequence [Fig. 4(a)] that removes the average ac Stark shift U_0. After applying $M = 48$ dressing pulses at a detuning $\Delta_* = 2\pi \times 8$ MHz and a central Rabi frequency $\Omega \approx 2\pi \times 1.2$ MHz, we measure the spin projection in a given quadrature $S_\alpha = S_z\cos(\alpha) + S_y\sin(\alpha)$ by performing a microwave rotation by an angle α about the mean spin vector $\langle S\rangle \propto \hat{\mathbf{x}}$ and reading out S_z via state-sensitive fluorescence imaging.

To quantify spin squeezing [Fig. 4(b)], we plot the Wineland parameter $\xi^2 = N\left(\Delta S_\alpha\right)^2 / \left|\langle \mathbf{S}\rangle\right|^2$, where $\xi^2 < 1$ indicates enhanced angular resolution due to entanglement [2]. Here, $|\langle \mathbf{S}\rangle|$ is the length of the total spin vector as determined from the contrast $\mathcal{C} = 2\left|\langle \mathbf{S}\rangle\right|/N$ of a Ramsey fringe. We calibrate the atom number N by measurements of the quantum projection noise of coherent spin states [54], where we remove a small amount of common-mode technical noise by a linear regression across microtraps. This same regression is applied to measurements of ΔS_α. The contrast is limited to $\mathcal{C}_0 = 0.95(1)$ by inhomogeneous trap light shifts that are imperfectly canceled by spin echo due to atomic motion. We choose a sufficiently short interaction time that the additional contrast loss due to the dressing light, including atom loss, is at most 1%.

To investigate the dependence of the squeezing on the interaction strength χ, we leverage the variation in intensity of the dressing light across the array. Figure 4(c) shows the minimum squeezing parameter $\xi^2_{\rm min} \equiv \xi^2(\alpha_{\rm opt})$ (green circles) for each of the nine array sites, compared with the value for the same quadrature in the absence of dressing light (gray squares). In addition, we plot an independent calibration of the twisting strength $Q \equiv \int \chi(t)\, dt$, based on the phase accumulated by coherent states $|\theta\rangle$ with different initial tilts in the full dressing sequence with spin echo [41, 54]. We observe the strongest squeezing in the array sites with the largest twisting strength, achieving a minimum squeezing parameter $\xi^2_{\rm min} = 0.77(9)$. We also observe correspondingly strong antisqueezing $\xi^2_{\rm max} \equiv \xi^2(\alpha_{\rm opt} - \pi/2)$ in the orthogonal quadrature (orange diamonds).

The dependence of squeezing and antisqueezing on twisting strength is summarized in Fig. 4(d). For comparison, the solid curves show a model of one-axis twisting with $N_c = 13$ neighbors, accounting for the finite baseline contrast $\mathcal{C}_0$. The squeezing and antisqueezing are consistent with the model predictions augmented by a small amount of technical noise. Our measurement includes all detection noise, which is on the scale of 3% of the quantum projection noise. Other factors contributing excess noise may include laser intensity fluctuations and residual effects of rare contaminant atoms.

The observed improvement in squeezing with increasing twisting strength suggests that stronger squeezing is attainable at higher laser intensity or longer interaction time. We limit the duration of each dressing pulse to $\tau_p \approx 600$ ns to avoid excess contrast loss attributable to contaminant atoms [54]. We also limit the total duration

of the stroboscopic dressing sequence to minimize trap-induced dephasing. This effect could be mitigated by improved cooling or state-insensitive trapping to access longer interaction times. In addition, higher intensity of the dressing light could be achieved by addressing the ensembles sequentially with a focused beam.

Stronger twisting will allow for observing limits to squeezing due to the finite interaction range. The inhomogeneous density of each atomic cloud is predicted to limit the squeezing to approximately $\xi^2_{\mathrm{inh}} = 0.3$ [27, 54] for our parameters. Overcoming this limit, either in an ordered array or in a shaped trapping potential, would enable squeezing by an amount $\xi_c^2 \propto N_c^{-2/3}$ set by the number of interacting neighbors. For example, in a fully three-dimensional system with the dressed interaction potential in this work, a uniform density $\rho = 2 \times 10^{11}$ cm^{-3} yields $N_c \approx 60$ and allows for squeezing by $\xi^2 \approx 0.09$, or equivalently $-10 \log \xi^2 \approx 10$ dB. The squeezing might further be improved by addition of a transverse field [29, 41] or by leveraging atomic motion to spread correlations beyond the interaction range.

By enabling local, optical control of spin squeezing in an array of atomic ensembles, Rydberg dressing is ideally suited to enhancing multiplexed atomic clocks and sensors. Prospective applications include clock comparisons for tests of fundamental physics [56], cascaded interrogation schemes for clocks limited by local oscillator noise [43, 45], and quantum-enhanced imaging of magnetic [15, 57] or electric [35] fields. The ability to access many-body entanglement by stroboscopic Rydberg dressing further promises to advance quantum simulations of lattice spin models that benefit from optical control of long-range interactions [27, 46, 58–61].

Note: During completion of this manuscript, we became aware of related works demonstrating spin squeezing using Rydberg interactions in two-dimensional arrays of single atoms [62, 63]. Bornet et al. [63] achieve a squeezing parameter $\xi^2 \approx 0.4$ via dipolar interactions among Rydberg atoms. Eckner et al. [62] demonstrate long-lived spin squeezing by Rydberg dressing in an optical clock, observing squeezing $\xi^2 \approx 0.4$ that saturates as the atom number is increased from $N = 4$ to $N = 70$. The authors attribute this saturation to collective dissipation, which might be mitigated by the stroboscopic dressing introduced here.

This work was supported by the ARO under grant numbers W911NF-20-1-0136 and W911NF-16-1-0490. We additionally acknowledge support from the AFOSR under grant No. FA9550-20-1-0059 (J. A. H. and N. A. L.), the National Defense Science and Engineering Graduate Fellowship (J. A. H.), the Stanford Science Fellowship (S. V. R.), the National Science Foundation Graduate Research Fellowship (G. L. M.), the ONR under grant No. N00014-17-1-2279 (O. M.), and the DOE Q-NEXT Quantum Center (M. S.-S.). We thank Adam Kaufman, Immanuel Bloch, Dan Stamper-Kurn, and Manuel Endres for stimulating discussions.

[1] M. Kitagawa and M. Ueda, Phys. Rev. A **47**, 5138 (1993).
[2] D. J. Wineland, J. J. Bollinger, W. M. Itano, and D. J. Heinzen, Phys. Rev. A **50**, 67 (1994).
[3] L. Pezzè, A. Smerzi, M. K. Oberthaler, R. Schmied, and P. Treutlein, Rev. Mod. Phys. **90**, 035005 (2018).
[4] I. D. Leroux, M. H. Schleier-Smith, and V. Vuletić, Phys. Rev. Lett. **104**, 073602 (2010).
[5] O. Hosten, R. Krishnakumar, N. J. Engelsen, and M. A. Kasevich, Science **352**, 1552 (2016).
[6] E. Pedrozo-Peñafiel, S. Colombo, C. Shu, A. F. Adiyatullin, Z. Li, E. Mendez, B. Braverman, A. Kawasaki, D. Akamatsu, Y. Xiao, and V. Vuletić, Nature **588**, 414 (2020).
[7] G. P. Greve, C. Luo, B. Wu, and J. K. Thompson, Nature **610**, 472 (2022).
[8] J. Estève, C. Gross, A. Weller, S. Giovanazzi, and M. K. Oberthaler, Nature **455**, 1216 (2008).
[9] C. Gross, T. Zibold, E. Nicklas, J. Estève, and M. K. Oberthaler, Nature **464**, 1165 (2010).
[10] M. F. Riedel, P. Böhi, Y. Li, T. W. Hänsch, A. Sinatra, and P. Treutlein, Nature **464**, 1170 (2010).
[11] B. Lücke, M. Scherer, J. Kruse, L. Pezzé, F. Deuretzbacher, P. Hyllus, O. Topic, J. Peise, W. Ertmer, J. Arlt, L. Santos, A. Smerzi, and C. Klempt, Science **334**, 773 (2011).
[12] C. D. Hamley, C. S. Gerving, T. M. Hoang, E. M. Bookjans, and M. S. Chapman, Nature Phys **8**, 305 (2012).
[13] T. Berrada, S. van Frank, R. Bücker, T. Schumm, J.-F. Schaff, and J. Schmiedmayer, Nat Commun **4**, 2077 (2013).
[14] C. F. Ockeloen, R. Schmied, M. F. Riedel, and P. Treutlein, Phys. Rev. Lett. **111**, 143001 (2013).
[15] W. Muessel, H. Strobel, D. Linnemann, D. B. Hume, and M. K. Oberthaler, Phys. Rev. Lett. **113**, 103004 (2014).
[16] V. Meyer, M. A. Rowe, D. Kielpinski, C. A. Sackett, W. M. Itano, C. Monroe, and D. J. Wineland, Phys. Rev. Lett. **86**, 5870 (2001).
[17] J. G. Bohnet, B. C. Sawyer, J. W. Britton, M. L. Wall, A. M. Rey, M. Foss-Feig, and J. J. Bollinger, Science **352**, 1297 (2016).
[18] T. Wilk, A. Gaëtan, C. Evellin, J. Wolters, Y. Miroshnychenko, P. Grangier, and A. Browaeys, Phys. Rev. Lett. **104**, 010502 (2010).
[19] Y.-Y. Jau, A. M. Hankin, T. Keating, I. H. Deutsch, and G. W. Biedermann, Nature Phys **12**, 71 (2016).
[20] J. Zeiher, R. van Bijnen, P. Schauß, S. Hild, J.-y. Choi, T. Pohl, I. Bloch, and C. Gross, Nat Phys **12**, 1095 (2016).
[21] A. Omran, H. Levine, A. Keesling, G. Semeghini, T. T. Wang, S. Ebadi, H. Bernien, A. S. Zibrov, H. Pichler, S. Choi, J. Cui, M. Rossignolo, P. Rembold, S. Montangero, T. Calarco, M. Endres, M. Greiner, V. Vuletić, and M. D. Lukin, Science **365**, 570 (2019).
[22] T. M. Graham, M. Kwon, B. Grinkemeyer, Z. Marra, X. Jiang, M. T. Lichtman, Y. Sun, M. Ebert, and M. Saffman, Phys. Rev. Lett. **123**, 230501 (2019).
[23] I. S. Madjarov, J. P. Covey, A. L. Shaw, J. Choi, A. Kale, A. Cooper, H. Pichler, V. Schkolnik, J. R. Williams, and

M. Endres, Nat. Phys. **16**, 857 (2020).
[24] L. I. R. Gil, R. Mukherjee, E. M. Bridge, M. P. A. Jones, and T. Pohl, Phys. Rev. Lett. **112**, 103601 (2014).
[25] I. Bouchoule and K. Mølmer, Phys. Rev. A **65**, 041803(R) (2002).
[26] T. Opatrný and K. Mølmer, Phys. Rev. A **86**, 023845 (2012).
[27] J. Van Damme, X. Zheng, M. Saffman, M. G. Vavilov, and S. Kolkowitz, Phys. Rev. A **103**, 023106 (2021).
[28] R. Kaubruegger, P. Silvi, C. Kokail, R. van Bijnen, A. M. Rey, J. Ye, A. M. Kaufman, and P. Zoller, Phys. Rev. Lett. **123**, 260505 (2019).
[29] J. T. Young, S. R. Muleady, M. A. Perlin, A. M. Kaufman, and A. M. Rey, arXiv:2208.01869 [quant-ph] (2022).
[30] T. Bilitewski, L. De Marco, J.-R. Li, K. Matsuda, W. G. Tobias, G. Valtolina, J. Ye, and A. M. Rey, Phys. Rev. Lett. **126**, 113401 (2021).
[31] S. D. Bennett, N. Y. Yao, J. Otterbach, P. Zoller, P. Rabl, and M. D. Lukin, Phys. Rev. Lett. **110**, 156402 (2013).
[32] K. Xia and J. Twamley, Phys. Rev. B **94**, 205118 (2016).
[33] M. A. Norcia, A. W. Young, W. J. Eckner, E. Oelker, J. Ye, and A. M. Kaufman, Science **366**, 93 (2019).
[34] I. S. Madjarov, A. Cooper, A. L. Shaw, J. P. Covey, V. Schkolnik, T. H. Yoon, J. R. Williams, and M. Endres, Phys. Rev. X **9**, 041052 (2019).
[35] A. Arias, G. Lochead, T. M. Wintermantel, S. Helmrich, and S. Whitlock, Phys. Rev. Lett. **122**, 053601 (2019).
[36] J. F. Barry, J. M. Schloss, E. Bauch, M. J. Turner, C. A. Hart, L. M. Pham, and R. L. Walsworth, Rev. Mod. Phys. **92**, 015004 (2020).
[37] A. Mitra, S. Omanakuttan, M. J. Martin, G. W. Biedermann, and I. H. Deutsch, arXiv.2205.12866 [quant-ph] (2022).
[38] G. Pupillo, A. Micheli, M. Boninsegni, I. Lesanovsky, and P. Zoller, Phys. Rev. Lett. **104**, 223002 (2010).
[39] J. E. Johnson and S. L. Rolston, Phys. Rev. A **82**, 033412 (2010).
[40] N. Henkel, R. Nath, and T. Pohl, Phys. Rev. Lett. **104**, 195302 (2010).
[41] V. Borish, O. Marković, J. A. Hines, S. V. Rajagopal, and M. Schleier-Smith, Phys. Rev. Lett. **124**, 063601 (2020).
[42] S. Hollerith, K. Srakaew, D. Wei, A. Rubio-Abadal, D. Adler, P. Weckesser, A. Kruckenhauser, V. Walther, R. van Bijnen, J. Rui, C. Gross, I. Bloch, and J. Zeiher, Phys. Rev. Lett. **128**, 113602 (2022).
[43] J. Borregaard and A. S. Sørensen, Phys. Rev. Lett. **111**, 090802 (2013).
[44] T. Rosenband and D. R. Leibrandt, arXiv:1303.6357 [quant-ph] (2013).
[45] E. M. Kessler, P. Kómár, M. Bishof, L. Jiang, A. S. Sørensen, J. Ye, and M. D. Lukin, Phys. Rev. Lett. **112**, 190403 (2014).
[46] J. Zeiher, J.-y. Choi, A. Rubio-Abadal, T. Pohl, R. van Bijnen, I. Bloch, and C. Gross, Phys. Rev. X **7**, 041063 (2017).
[47] E. Guardado-Sanchez, B. M. Spar, P. Schauss, R. Belyansky, J. T. Young, P. Bienias, A. V. Gorshkov, T. Iadecola, and W. S. Bakr, Phys. Rev. X **11**, 021036 (2021).
[48] E. A. Goldschmidt, T. Boulier, R. C. Brown, S. B. Koller, J. T. Young, A. V. Gorshkov, S. L. Rolston, and J. V. Porto, Phys. Rev. Lett. **116**, 113001 (2016).
[49] J. A. Aman, B. J. DeSalvo, F. B. Dunning, T. C. Killian, S. Yoshida, and J. Burgdörfer, Phys. Rev. A **93**, 043425 (2016).
[50] T. Boulier, E. Magnan, C. Bracamontes, J. Maslek, E. A. Goldschmidt, J. T. Young, A. V. Gorshkov, S. L. Rolston, and J. V. Porto, Phys. Rev. A **96**, 053409 (2017).
[51] B. J. DeSalvo, J. A. Aman, C. Gaul, T. Pohl, S. Yoshida, J. Burgdörfer, K. R. A. Hazzard, F. B. Dunning, and T. C. Killian, Phys. Rev. A **93**, 022709 (2016).
[52] J. T. Young, T. Boulier, E. Magnan, E. A. Goldschmidt, R. M. Wilson, S. L. Rolston, J. V. Porto, and A. V. Gorshkov, Phys. Rev. A **97**, 023424 (2018).
[53] L. Festa, N. Lorenz, L.-M. Steinert, Z. Chen, P. Osterholz, R. Eberhard, and C. Gross, Phys. Rev. A **105**, 013109 (2022).
[54] See Supplemental Material, which includes Refs. [64–71], for additional experimental details and supporting derivations.
[55] S. K. Dutta, J. R. Guest, D. Feldbaum, A. Walz-Flannigan, and G. Raithel, Phys. Rev. Lett. **85**, 5551 (2000).
[56] X. Zheng, J. Dolde, V. Lochab, B. N. Merriman, H. Li, and S. Kolkowitz, Nature **602**, 425 (2022).
[57] F. Yang, S. F. Taylor, S. D. Edkins, J. C. Palmstrom, I. R. Fisher, and B. L. Lev, Nat. Phys. **16**, 514 (2020).
[58] A. W. Glaetzle, M. Dalmonte, R. Nath, I. Rousochatzakis, R. Moessner, and P. Zoller, Phys. Rev. X **4**, 041037 (2014).
[59] A. W. Glaetzle, M. Dalmonte, R. Nath, C. Gross, I. Bloch, and P. Zoller, Phys. Rev. Lett. **114**, 173002 (2015).
[60] I.-D. Potirniche, A. C. Potter, M. Schleier-Smith, A. Vishwanath, and N. Y. Yao, Phys. Rev. Lett. **119**, 123601 (2017).
[61] L.-M. Steinert, P. Osterholz, R. Eberhard, L. Festa, N. Lorenz, Z. Chen, A. Trautmann, and C. Gross, arXiv:2206.12385 [physics.atom-ph] (2022).
[62] W. J. Eckner, N. D. Oppong, A. Cao, A. W. Young, W. R. Milner, J. M. Robinson, J. Ye, and A. M. Kaufman, arXiv:2303.08078 [quant-ph] (2023).
[63] G. Bornet, G. Emperauger, C. Chen, B. Ye, M. Block, M. Bintz, J. A. Boyd, D. Barredo, T. Comparin, F. Mezzacapo, T. Roscilde, T. Lahaye, N. Y. Yao, and A. Browaeys, arXiv:2303.08053 [quant-ph] (2023).
[64] T. Gullion, D. B. Baker, and M. S. Conradi, Journal of Magnetic Resonance (1969) **89**, 479 (1990).
[65] N. Šibalić, J. D. Pritchard, C. S. Adams, and K. J. Weatherill, Computer Physics Communications **220**, 319 (2017).
[66] M. Foss-Feig, K. R. A. Hazzard, J. J. Bollinger, and A. M. Rey, Phys. Rev. A **87**, 042101 (2013).
[67] O. Hosten, N. J. Engelsen, R. Krishnakumar, and M. A. Kasevich, Nature **529**, 505 (2016).
[68] K. C. Cox, G. P. Greve, J. M. Weiner, and J. K. Thompson, Phys. Rev. Lett. **116**, 093602 (2016).
[69] S. Colombo, E. Pedrozo-Peñafiel, A. F. Adiyatullin, Z. Li, E. Mendez, C. Shu, and V. Vuletić, Nat. Phys. **18**, 925 (2022).
[70] E. Davis, G. Bentsen, and M. Schleier-Smith, Phys. Rev. Lett. **116**, 053601 (2016).
[71] T. Macrì, A. Smerzi, and L. Pezzè, Phys. Rev. A **94**, 010102(R) (2016).